

ARTICLE

Evaluating UAV-based multispectral imagery for mapping an intertidal seagrass environment

Eylem Elma¹  | Rachel Gaulton¹ | Thomas R. Chudley²  | Catherine L. Scott³ | Holly K. East⁴ | Hannah Westoby⁵ | Clare Fitzsimmons¹

¹School of Natural and Environmental Sciences, Newcastle University, Newcastle upon Tyne, UK

²Department of Geography, Durham University, Durham, UK

³Natural England, Lancaster House, Newcastle upon Tyne, UK

⁴Department of Geography and Environmental Sciences, Faculty of Engineering and Environment, Northumbria University, Newcastle upon Tyne, UK

⁵Environment Agency, Newcastle upon Tyne, UK

Correspondence

Eylem Elma, School of Natural and Environmental Sciences, Newcastle University, Newcastle upon Tyne, UK.

Email: e.elma2@newcastle.ac.uk

Funding information

Natural Environment Research Council (NERC) via the ONE Planet DTP, Grant/Award Number: NE/S007512/1; Natural England, UK

Abstract

1. Worldwide seagrass habitats are under severe anthropogenic threat. In the United Kingdom (UK), the health of habitats of the widely distributed *Zostera* species is particularly threatened by eutrophication that can lead to detrimental macroalgae overgrowth. To manage and conserve seagrass habitats, effective monitoring tools are required.
2. We use an off-the-shelf consumer-grade multispectral (RGB, red edge, and near-infrared) camera mounted on an unoccupied aerial vehicle (UAV) to map an intertidal multispecies seagrass environment in Lindisfarne National Nature Reserve, Northumberland, UK.
3. Field surveys were undertaken of three seagrass areas, including those dominated by *Zostera noltii*, *Zostera marina* and macroalgae. Using the Maximum Likelihood Classifier (MLC), results indicated an overall accuracy (OA) between 84% and 91% across classified habitat maps. As expected, the red edge and near-infrared bands offered an advantage beyond RGB imagery to discriminate between the vegetation types for accurate habitat mapping.
4. Our research provides a foundation for accurately mapping a complex intertidal seagrass environment through the utilisation of an off-the-shelf multispectral UAV. The study may aid the implementation and development of effective monitoring programmes for the management of *Zostera* spp. decline and macroalgae proliferation to prevent seagrass degradation and conserve these valuable yet fragile ecosystems.

KEYWORDS

habitat classification, intertidal mapping, macroalgae, multispectral UAV, remote sensing, seagrass

1 | INTRODUCTION

Seagrass ecosystems globally are facing ongoing decline due to increasing anthropogenic and natural impacts, such as nutrient input,

coastal development, destructive fishing practices and climate change (Dunic et al., 2021; Turschwell et al., 2021; Waycott et al., 2009). An estimated 30% of seagrass habitats worldwide have vanished since the late nineteenth century, and at least 22 seagrass species are in

This is an open access article under the terms of the [Creative Commons Attribution](https://creativecommons.org/licenses/by/4.0/) License, which permits use, distribution and reproduction in any medium, provided the original work is properly cited.

© 2024 The Author(s). *Aquatic Conservation: Marine and Freshwater Ecosystems* published by John Wiley & Sons Ltd.

decline (United Nations Environment Programme, UNEP, 2020). Recent studies have raised particular concern about declines in the widely distributed seagrass species, *Zostera* spp., along the United Kingdom's (UK) coastlines (Jones & Unsworth, 2016). For example, Green et al. (2021) showed that at least 39% of the UK's seagrass habitat area has been lost since the 1980s and that this loss is accelerating. The loss of *Zostera* spp. habitats can have a significant impact on feeding grounds for internationally protected migratory birds (e.g., Light-Bellied Brent Geese) (Clausen et al., 2012; Ganter, 2000), loss of essential fish habitat for many commercially important fish species (Bertelli & Unsworth, 2014; Polte & Asmus, 2006), and reduced carbon sequestration (Gao et al., 2022; Röhr et al., 2018; Zou et al., 2021). Hence, *Zostera* spp. habitats support a much broader conservation agenda, as critical ecosystem functions and the services they provide are being lost (Hughes et al., 2009; Orth et al., 2006).

A particular threat faced by UK seagrasses is poor water quality leading to eutrophication (i.e., nutrient enrichment from land) (Jones et al., 2018; Jones & Unsworth, 2016; Maier et al., 2009). In turn, this can encourage the proliferation of macroalgae, which is detrimental to *Zostera* spp. due to overshadowing, smothering and, ultimately, the suppression of seagrass growth (Burkholder et al., 2007; Cardoso et al., 2004; Hauxwell et al., 2001). To better understand ecosystem processes and dynamics of *Zostera* spp. habitats, effective monitoring programmes are needed (Jones & Unsworth, 2016; Strachan et al., 2022), particularly those that accurately assess spatiotemporal changes in the presence and distribution of *Zostera* spp. and opportunistic macroalgae (Hobley et al., 2021). Such information is critical to the detection of algal cover and overgrowth and essential for the development of management strategies to safeguard, restore and prevent seagrass habitat degradation (Unsworth et al., 2022, 2019; Ventura et al., 2022).

While conventional in situ field methods are well established, these are often expensive, time-consuming and lack accurate spatiotemporal information. Optical remote sensing methods, in comparison, have been demonstrated to be useful for the mapping and monitoring of seagrass habitats cost-effectively, assessing large areas rapidly, and with high repeatability (Hossain et al., 2015; Veettil et al., 2020). In recent years, unoccupied aerial vehicles (UAV) have gained increased attention for application in seagrass habitat mapping and monitoring (e.g., Price et al., 2022; Ventura et al., 2018; Yang et al., 2020). Their utilisation has been successful in intertidal (Duffy et al., 2018; Yang et al., 2023) and subtidal (Nahirnick, Hunter, et al., 2019; Nahirnick, Reshitnyk, et al., 2019; Prystay et al., 2023) seagrass environments, since they offer affordable ways of acquiring very high resolution images and fill important gaps in remote sensing capability in temporally dynamic and complex environments with a potential to revolutionise the toolbox of coastal managers (Bremner et al., 2023; Doukari & Topouzelis, 2022).

Specific benefits of UAVs in comparison to other optical remote sensing technology (e.g., satellite imagery) for monitoring programmes include (1) very high spatial resolution, which increases the ability to capture detailed features in imagery permitting identification of

seagrass species and other benthic organisms (Duffy et al., 2018; James et al., 2020); (2) control of temporal resolution as appropriate weather conditions for image acquisitions can be chosen; (3) coverage of areas inaccessible on the ground; (4) relatively small, portable and user-friendly; and (5) customised and repeatable flight planning is possible as flight paths can be saved making data acquisition reproducible to enable repetitive inventories, relevant to monitoring programmes (Nahirnick, Hunter, et al., 2019; Nahirnick, Reshitnyk, et al., 2019). To effectively map and monitor seagrass environments that contain multiple vegetation taxa with similar spectral properties (i.e., *Zostera* spp. and green macroalgae), higher spectral resolution sensors are required. Such sensors may enable discrimination and permit accurate habitat mapping (Davies et al., 2023).

The vulnerability of different seagrass species to threats and their response to environmental changes can be different, such as varying tolerance thresholds to temperature fluctuations and nutrient levels, impacting survival to varying degrees (Grech et al., 2012; Kaldy, 2014; la Nafie et al., 2012; Massa et al., 2009). Additionally, seagrass species may differ in their provision of ecosystem services and functioning such as efficiency in carbon storage (Postlethwaite et al., 2018; Sousa et al., 2019), their suitability as a habitat for many threatened seagrass dependent species and commercially important fish species (Bertelli & Unsworth, 2014; Hughes et al., 2009). Therefore, management may need to vary by species. To meet species-specific management and conservation goals, accurate identification of species and spatial distributions are required to enable coastal managers to make informed decisions when prioritising areas for protection (Wilson et al., 2005).

In temperate seagrass meadows, most studies to date have used consumer-grade UAVs with either limited spectral resolutions, for example, simple red-green-blue (RGB) or five-band multispectral cameras (RGB, red edge, and near-infrared). These have successfully mapped monospecific seagrass habitats, with a focus on the presence/absence and/or density of seagrass cover (Chand & Bollard, 2021; Duffy et al., 2018; Martin et al., 2020; Svane et al., 2022), but few have disaggregated more complex vegetative habitats (Hobley et al., 2021; Tahara et al., 2022). For instance, Tahara et al. (2022) utilised RGB UAV imagery for mapping co-occurring seagrass and algal species in an intertidal seagrass habitat in Japan, while some other studies have also used multispectral UAV cameras to discriminate between vegetation taxa (i.e., seagrass and macroalgae) in temperate intertidal areas. Román et al. (2021) used a MicaSense RedEdge-MX dual 10-band multispectral camera to map the only presence of *Zostera noltii* in the intertidal area and the seagrass species *Cymodocea nodosa* and green macroalgae in the subtidal area (submerged). In contrast, Hobley et al. (2021) used a MicaSense RedEdge 3 multispectral camera and successfully mapped and discriminated algal species in a multispecies intertidal seagrass environment, but no discrimination was made between seagrass species. In addition, available studies have used computationally intensive analysis (e.g., deep learning; Hobley et al., 2021) or required a high number of spectral bands (up to 10) to achieve accurate map outputs (Román et al., 2021). This requires cameras that need to be custom mounted on the UAV, increasing operational costs. With improving UAV technology, affordable off-the-

shelf consumer-grade UAVs that are equipped with multispectral cameras have recently become available, which may simplify logistics and analysis and support management actions. However, their application and efficacy in mapping complex heterogeneous intertidal seagrass environments still require testing, to develop a foundation and guidelines for coastal managers and effective conservation of seagrass habitats.

Here, we propose using an off-the-shelf consumer grade UAV equipped with a multispectral camera (Phantom 4 RTK multispectral) to create habitat maps of highly mixed and complex intertidal multispecies seagrass environment exposed at low tide in North East, UK. We used a pixel-based classification method to evaluate the ability of a five-band (RGB, red edge, and near-infrared) multispectral camera to discriminate between *Zostera* spp. (*Zostera noltii* and *Zostera marina*, respectively) and opportunistic green macroalgae on three transects with varying benthic community composition. Classification was validated using detailed field survey data. The accuracies of classifications that used multispectral and RGB-only

data were compared, with a view to assessing the operational need for multispectral imagery for seagrass mapping. We discuss field logistics and the operational potential of UAV utilisation for intertidal seagrass habitat monitoring, with a view to moving such methods towards operational use.

2 | METHODS AND MATERIALS

2.1 | Field site

The study was performed in the Causeway area within the Lindisfarne National Nature Reserve (LNNR), Northumberland, UK (Figure 1). The field site is an intertidal mudflat and sandflat, which is exposed during low tide and consists of sparse to dense *Zostera* spp. habitats. Two seagrass species, *Z. noltii* and *Z. marina*, were present in the field. *Z. noltii* is the dominant species and can form large dense meadows across the site. Other benthic substrates such as sand, lugworm casts

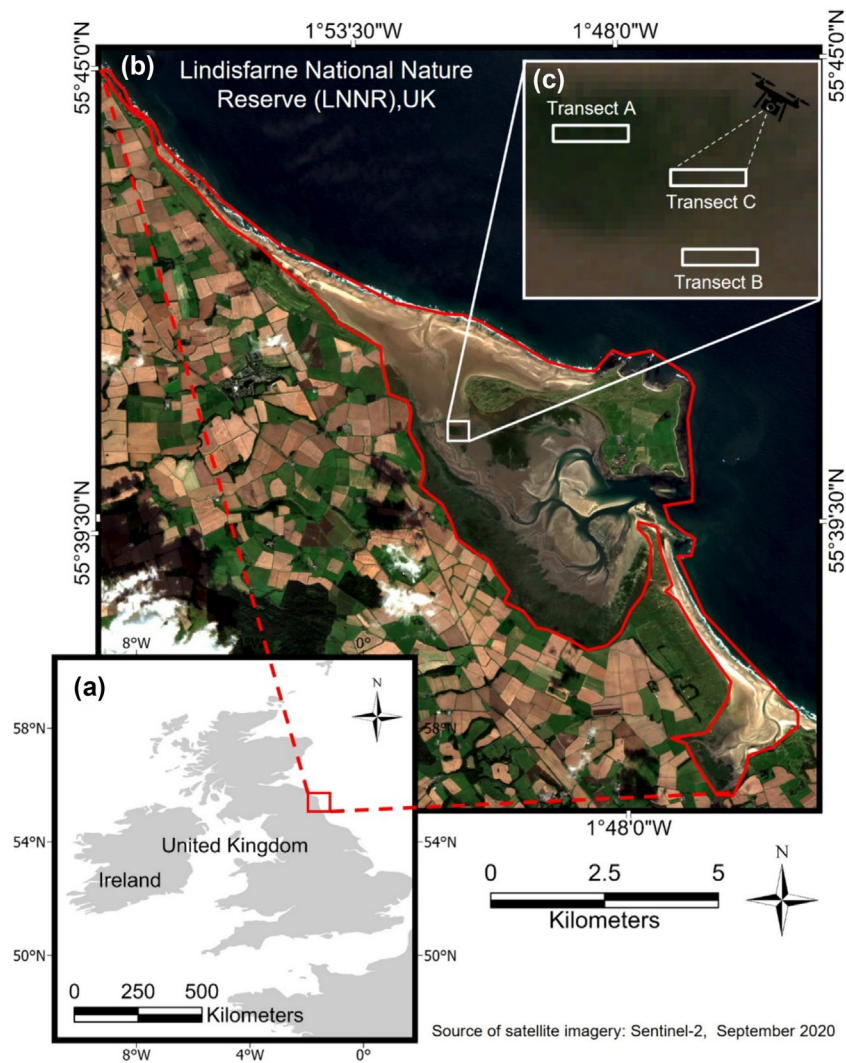


FIGURE 1 (a) Map of the UK showing the location of Lindisfarne National Nature Reserve (LNNR) (red square), (b) LNNR (red boundary outline) indicating the field survey area (white square) and (c) the flight transects surveyed in this study. Transect A, *Zostera noltii* dominated; Transect B, *Zostera marina* dominated; Transect C, Macroalgae dominated.

and a mixed complex of opportunistic green macroalgae such as *Enteromorpha* (*Ulva intestinalis*; macroalgae hereafter) were also present.

2.2 | Equipment specifications

A DJI Phantom 4 Multispectral Real-Time Kinematic (RTK) UAV was used to perform flight missions. The UAV has a camera attached that consists of five in-built 1/1.29" CMOS monochrome sensors with an image size of 1,600 × 1,300 pixels (2.02 MP) including the following bands: blue (B: 450 nm ± 16 nm), green (G: 560 nm ± 16 nm), red (R: 650 nm ± 16 nm), red edge (RE: 730 nm ± 16 nm) and near-infrared (NIR: 840 nm ± 26 nm). The aircraft includes a spectral sunlight sensor to detect solar irradiance, which allows reflectance calibration of images. Flight planning was conducted using the DJI Ground Station Pro app (v. 2.0.16) that enabled pre-preparation of flight settings. A Labsphere SRT-99-100 Spectralon Diffuse Reflectance Target calibration panel was used for radiometric calibration. The panel was calibrated, and the data were provided by the Natural Environment Research Council Field Spectroscopy Facility (NERC FSF). Prior to flights, images of the reflectance panel were taken with the UAV camera. These images were then used in the imagery pre-processing stage.

2.3 | UAV and ground-truth survey

Flight missions were conducted around seagrass peak biomass on 24 August 2021, during exposed low tide, to minimise the effect of surface water. Three 100 m × 20 m transects (2,000 m²) were surveyed, with each survey taking approximately 19 min flight time.

Images were captured at 10 m altitude with a 5.4 mm/pixel spatial resolution, using a 70% side and fore overlap at an equal distance interval within the 2D mode. An off-nadir angle, with a gimbal pitch of −80° was used. The geographic position of the camera was established using the fitted RTK GNSS corrected against a DJI D-RTK 2 base station service. The location of each transect was selected based on species coverage and composition to capture widespread heterogeneous vegetated areas. Transects constituting the three different dominant vegetation types were then surveyed: *Z. noltii* dominated (55°40'39"N 1°51'29"W), *Z. marina* dominated (55°40'34"N 1°51'19"W) and macroalgae dominated (55°40'37"N 1°51'21"W) (Transects A–C, respectively, as we refer to them hereafter) (Figure 1).

To train and validate UAV images, photographs of 1m² ground quadrats were taken immediately on the ground after flight missions. In total, 20 quadrat photographs were taken at predefined regular intervals every 10 m across two rows within the flight transect, resulting in a total number of 60 quadrats across all transects (Figure 2a). A smartphone with the Google Earth Pro app was used to allow the field team to navigate to the coordinates of predefined quadrat sampling points. To enable geolocation of quadrats for the purpose of georeferencing in the analysis stage, GPS positions of the north and south corners of each quadrat were taken using a Trimble Catalyst receiver with the Trimble Network RTK Precision service (±0.2 cm accuracy) (Figure 2b).

2.4 | Image pre-processing

Agisoft Metashape (v. 1.7.3) was used to create orthomosaics using TIFF files acquired by the UAV. Prior to processing, the quality of images was checked. The image quality assessment is scaled between

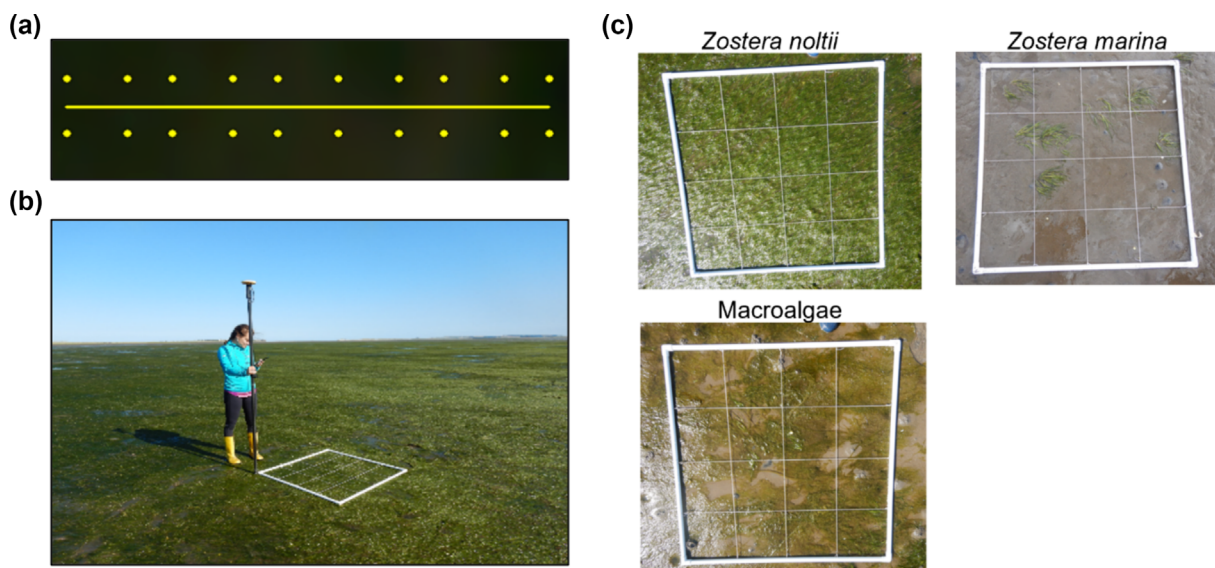


FIGURE 2 (a) Flight transect showing the predefined regular points for photoquadrats ($n = 20$) across a flight transect. (b) Image showing the quadrat and a Trimble receiver to record the northern corner of the quadrat sample. (c) Photographs of a *Zostera noltii*, *Zostera marina* and Macroalgae dominated quadrats.

0 and 1 (unitless), whereby the quality assessment value of 1 corresponds to the highest possible image quality. Images were considered based on an image quality value of >0.5 , to facilitate the removal of blurred imagery (Agisoft, 2021; Over et al., 2021). To calibrate reflectance, panel calibration data provided by NERC FSF were resampled to the sensor spectral bands by assigning calibrated reflectance to the five band wavelengths of UAV images using the *Calibrate Reflectance* tool. Prior to conducting the reflectance calibration, calibration images were masked so that only the reflectance panel area was marked. Sun sensor data were also used within the calibration to account for the Sun's position and irradiance and improve the accuracy of the reflectance calibration process. Photo alignment and sparse cloud generation were performed using the highest accuracy setting, a key point limit of 40,000 and a zero-tie point limit. Afterwards, low-quality tie points within the generated sparse cloud point were selected and removed by filtering by reconstruction uncertainty, projection uncertainty and projection error. Error was reduced by iteratively selecting and deleting points and re-optimising the camera after each removal. This procedure was performed manually until the self-reported standard error of unit weight (SEUW) was close

to 1 (Over et al., 2021). Afterwards, a dense cloud was created, which was followed by the generation of a digital elevation model (DEM). The DEM was used to create an orthomosaic for each individual band. Pixel reflectance values ranging from 0–1 were generated by dividing the measured reflectance value of each band by normalisation factor, in this case 32,768, the middle of the available range of 16-bit integers (e.g., B1/32768).

2.5 | Training data and image classification

Quadrat photographs were aligned with the orthomosaic, using ArcGIS (v.10.6.1) to aid in the assignment of habitat classes. Afterwards, based on visual assessment of photoquadrats, regions of interest (ROIs/pixels) were created randomly within each quadrat area, using ENVI (v.5.6.2). Where certain benthic classes were not found sufficiently within the quadrat sampling areas, random samples were created outside of the quadrat. Pixels were assigned to the following benthic classes: *Z. noltii*, *Z. marina*, macroalgae, bare ground, lugworm casts, decomposing vegetation, anoxic sediment, and decomposing vegetation, anoxic sediment,

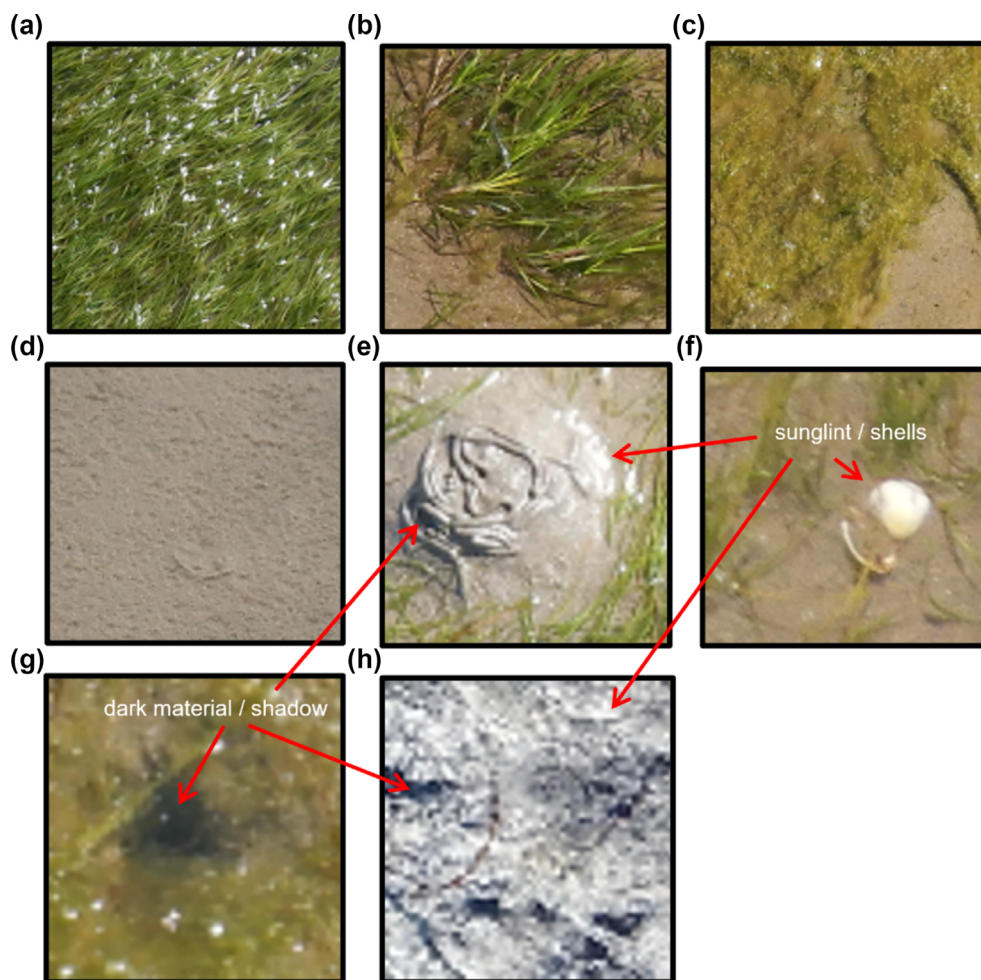


FIGURE 3 Images of benthic substrates initially identified in quadrat photographs before aggregation of benthic classes in further analysis. (a) *Zostera noltii*, (b) *Zostera marina*, (c) macroalgae, (d) bare ground, (e) lugworm casts, (f) shells, (g) anoxic sediment and (h) decomposing vegetation. Arrows highlight examples of categories including dark material/shadow and sunglint/shells.

shadow (i.e., from leaves or part of lugworm casts), sunglint and shells (Figure 3). The primary interest of this study was in mapping the vegetation species. Therefore, benthic substrates other than vegetation (i.e., bare ground, lugworm casts, decomposing vegetation, anoxic sediment, shadow, sunglint and shells) were compiled into two classes with similar spectral reflectance. Anoxic sediment, shadow and dark areas within the decomposing vegetation substrate were compiled into the class, dark material/shadow, respectively. Sunglint, shells and white areas within the decomposing vegetation substrate were compiled into the class, sunglint/shells, respectively (Figure 3e–h). This resulted in a total of six benthic classes: *Z. noltii*, *Z. marina*, macroalgae, bare ground, dark material/shadow and sunglint/shells, respectively (Figure 3e–h). The data were then split into two sets of 50% for each: 50% for training the classification algorithm and the remaining 50% for validation of classified map output.

The Jeffries-Matusita (J-M) distance measure, a widely used measure for spectral discrimination of vegetation types (Schmidt & Skidmore, 2003), was applied using ENVI (v.5.6.2) to assess the statistical separation between created ground-truth classes (Richards, 2013). The J-M index value ranges between 0 and 2, whereby a 0 value indicates a complete overlap of spectral signatures and a value of 2 a complete separation of spectral signatures between two classes. To evaluate the strength of separation between classes, the following values were used: poor ($0.0 < x < 1.0$), moderate ($1.0 < x < 1.9$) and good separability ($1.9 < x < 2.0$).

The Maximum Likelihood Classifier (MLC), a supervised pixel-based classification method that uses spectral information to assign pixels to habitat classes, was employed in ENVI (v.5.6.2) for benthic habitat classification. The classifier is based on the assumption that each training class follows a normal distribution. It considers the mean and covariance of the training class signature when assigning

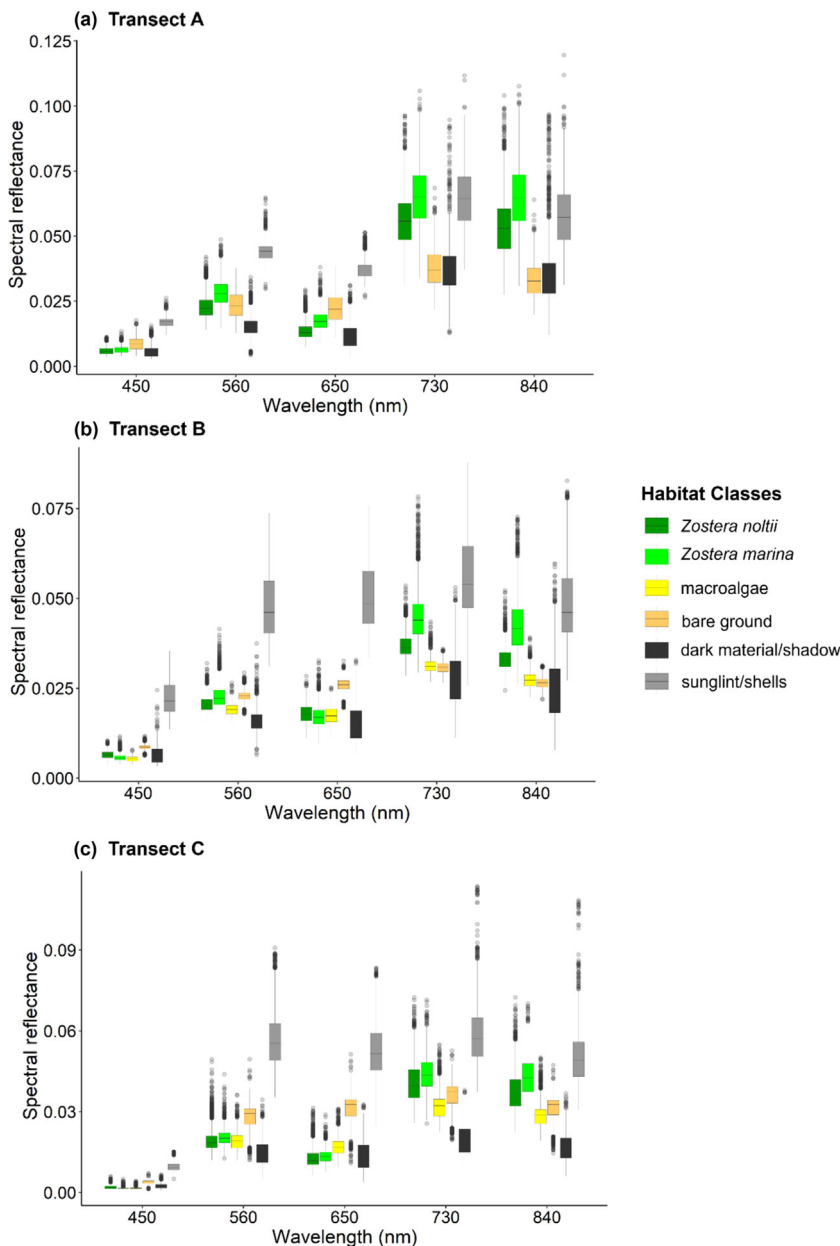


FIGURE 4 Spectral signatures of generated training data including all benthic classes across the multispectral bands for (a) Transect A (*Zostera noltii* dominated), (b) Transect B (*Zostera marina* dominated) and (c) Transect C (Macroalgae dominated). Boxplots show the median value (horizontal line), the interquartile range representing the dispersion of the data (size of the box), the upper and lower quartiles and outliers.

pixels to each class. The selection of this classifier was based on the dataset meeting normality assumptions and its proven success and reliability of application in seagrass habitats often outperforming other classifiers (e.g., Román et al., 2021). MLC is also widely available as a classifier in multiple commercial and open-source geospatial and image processing software, increasing its availability for operational applications. To evaluate the operational need for accurate multi-species habitat mapping, a comparison of the accuracy classification between an RGB and multispectral imagery was made. Here, the MLCs were trained on three bands (RGB) and five bands (RGB, red edge, and near-infrared) for each transect separately.

2.6 | Accuracy assessment

A confusion matrix was generated to assess the accuracy of the classified habitat maps (Congalton & Green, 2008). The overall accuracy (OA) gives information about the percentage of the total number of pixels contained within the ground truth area that have been correctly classified by the classification. User's accuracy (UA) and producer's accuracy (PA) then permit the assessment of the accuracy of each individual class. The confusion matrix outputs will be used to identify the nature of misclassifications between habitat classes.

3 | RESULTS

3.1 | Training data separability

While the spectral separation between all recorded benthic substrates was least within the blue band, benthic classes, including bare ground,

sunglint/shells and dark material/shadow, appeared to be separable from vegetation across nearly all bands. However, the multispectral sensor showed the least separability between *Z. noltii*, *Z. marina* and macroalgae across the red-green-blue (RGB) bands and a distinct separation between these vegetation types within the red edge (RE) and near-infrared (NIR) bands (Figure 4). When considering all spectral bands to investigate spectral separability of the training data of benthic classes, Jeffries–Matusita's separability values indicated the lowest pair separation between the two seagrass species, *Z. noltii* and *Z. marina*, among all vegetation species, for all three transects (Table 1). Respectively, Transects A and B showed lower separability (J-M value: 0.9 and 1.0, respectively), compared to Transect C (J-M value: 1.3). Where macroalgae was present in the image, that is, Transects B and C, results indicated a moderate pair separation between the two seagrass species and macroalgae (J-M value: ranging between 1.4 and 1.7). All pairwise separation values between the vegetation species and the other benthic categories indicated moderate to good separability (Table 1).

3.2 | Maximum Likelihood classification and accuracy assessment

Using the Maximum Likelihood Classifier (MLC), detailed benthic maps were produced (Figure 5) with higher overall accuracy (OA) when considering all five spectral bands (multispectral image) in comparison to RGB only bands (Table 2). The lowest accuracy was found for the Transect A classified map with an OA of 84% for the multispectral image and 57% OA for the RGB image. Transects B and C maps indicated very high OA for the multispectral image (91% and 89%, respectively) and lower OA for the RGB image (63% and 72%,

TABLE 1 Results of Jeffries–Matusita index, indicating spectral pair separability based on five spectral bands of benthic classes for Transect A (*Zostera noltii* dominated), Transect B (*Zostera marina* dominated) and Transect C (Macroalgae dominated). Where a class was not present in a transect to conduct pair separability, these were marked with NA, not available.

Benthic pair classes		Transect A	Transect B	Transect C
<i>Z. noltii</i>	<i>Z. marina</i>	0.9	1	1.3
<i>Z. noltii</i>	macroalgae	NA	1.7	1.4
<i>Z. marina</i>	macroalgae	NA	1.6	1.7
<i>Z. noltii</i>	dark material/shadow	1.4	1.7	1.7
macroalgae	dark material/shadow	NA	1.8	1.9
bare ground	dark material/shadow	1.5	1.9	2
<i>Z. marina</i>	dark material/shadow	1.6	1.9	1.7
bare ground	sunglint/shells	1.8	2	2
<i>Z. noltii</i>	bare ground	1.8	2	2
<i>Z. marina</i>	bare ground	1.9	2	2
<i>Z. marina</i>	sunglint/shells	1.9	2	2
sunglint/shells	dark material/shadow	1.9	1.9	2
<i>Z. noltii</i>	sunglint/shells	2	2	2
macroalgae	bare ground	NA	2	2
macroalgae	sunglint/shells	NA	2	2

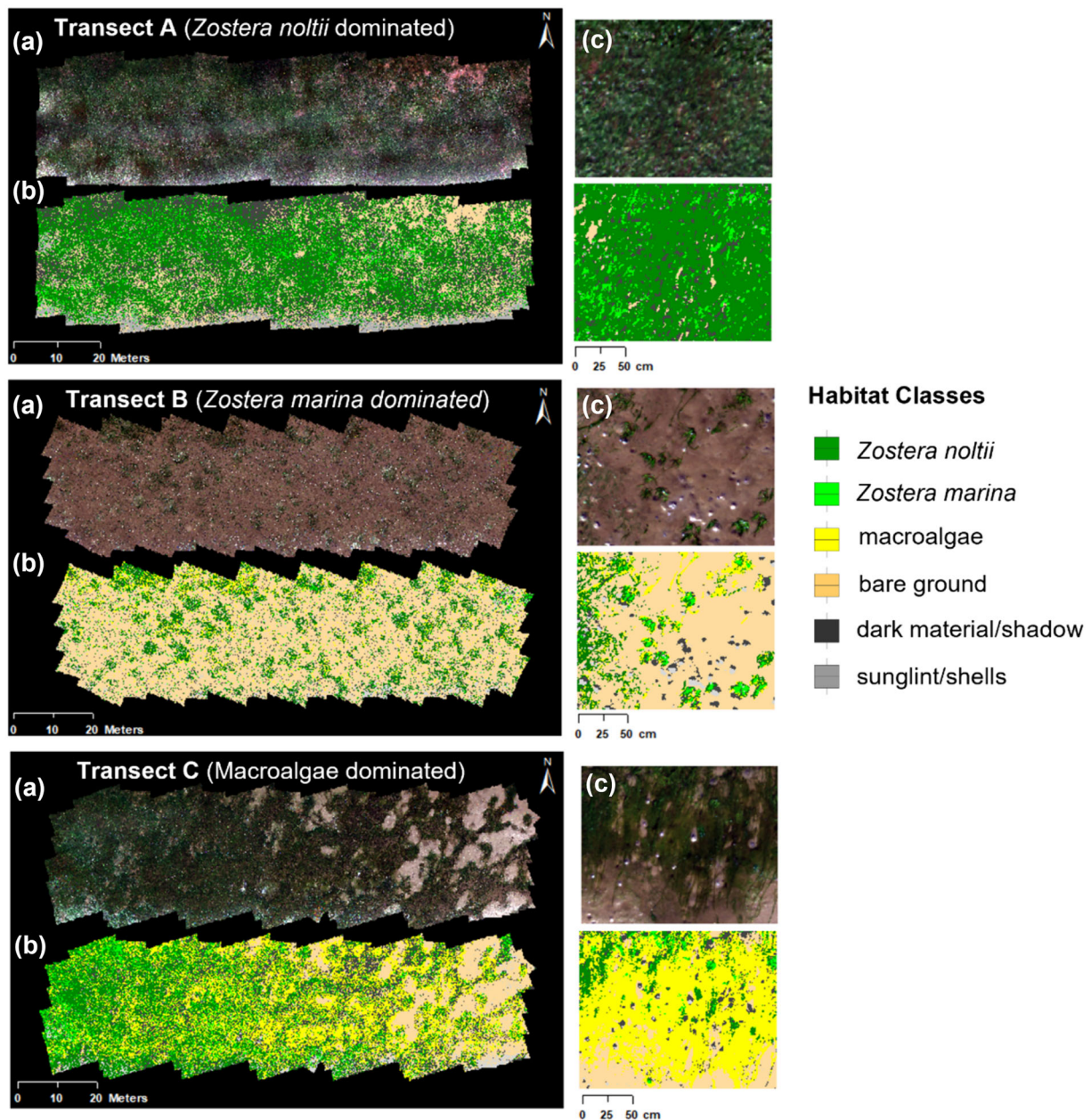


FIGURE 5 (a) Raw multispectral UAV orthomosaic are displayed using the red, green and blue colour composite; (b) classified map using Maximum Likelihood Classifier (MLC); and (c) a close-up example for each transect survey. Transect A, *Zostera noltii* dominated; Transect B, *Zostera marina* dominated; Transect C, Macroalgae dominated.

respectively) (Table 2). Considering the multispectral images only, class level accuracy for each transect map indicated a general pattern of lower PA and UA for all vegetation classes (*Z. noltii*, *Z. marina* and Macroalgae, respectively) in comparison to non-vegetation classes (bare ground, sunglint/shells and dark material/shadow, respectively). Vegetation classes indicated PA and UA ranging between 73% and 99%, and non-vegetation classes indicated PA and UA ranging between 79% and 100% in all transect maps (Table 2), except for distinctly lower UA values for the macroalgae class (UA 54%) in the Transect B map, which may be due to small sample size because of its sparse representation in the studied transect area, and PA for dark material/shadows (64%) in the Transect A map, due to small validation sample size.

Similar to J-M results for training data, the post-classification accuracy assessment results indicated notably higher misclassification among vegetation classes in comparison to all other benthic classes, across all classified transect maps. The largest misclassification among habitat classes was found between *Z. noltii* and *Z. marina*. In Transect A, 24.7% proportion of sampled pixels of *Z. noltii* was incorrectly classified as *Z. marina* class, and 6.7% of the class *Z. marina* was incorrectly classified as *Z. noltii*. Transect B indicated a lower misclassification of sampled pixels of *Z. noltii* as *Z. marina* (13% proportion of sampled pixels), and only 2% of *Z. marina* pixels were incorrectly classified as *Z. noltii* class. Finally, Transect C indicated 14.8% of sampled pixels of *Z. noltii* as *Z. marina*, and similarly, 14.7%

TABLE 2 Post-classification analysis showing the accuracy assessment outputs of the Maximum Likelihood classification map for (a) the multispectral image and (b) the RGB image. Transect A, *Zostera noltii* dominated; Transect B, *Zostera marina* dominated; Transect C, Macroalgae dominated.

(a) Overall accuracy (OA)	Transect A		Transect B		Transect C	
	Producer's accuracy (%)	User's accuracy (%)	Producer's accuracy (%)	User's accuracy (%)	Producer's accuracy (%)	User's accuracy (%)
Habitat classes						
<i>Zostera noltii</i>	90	80	84	85	76	80
<i>Zostera marina</i>	73	84	82	87	80	73
macroalgae	-	-	87	54	99	91
bare ground	90	92	100	99	100	98
dark material/ shadow	64	79	92	99	90	96
sunlint/shells	95	84	99	97	100	93
(b) Overall accuracy (OA)	57%		63%		72%	
Habitat classes						
<i>Zostera noltii</i>	61	68	56	61	40	56
<i>Zostera marina</i>	37	54	57	68	54	65
macroalgae	-	-	37	9	59	71
bare ground	86	55	77	72	93	70
dark material/ shadow	33	46	68	86	81	76
sunlint/shells	67	39	69	87	94	85

of *Z. marina* pixels were incorrectly classified as *Z. noltii*. Misclassification between macroalgae and *Zostera* spp. was notably lower in transects where macroalgae was present (Transects B and C, respectively). In both transects, between 4% to 9% of macroalgae pixels were incorrectly classified as *Z. noltii* or *Z. marina*, whereas up to 10% of *Z. noltii* pixels and 2% *Z. marina* pixels were incorrectly classified as macroalgae. Other notable misclassification was found between *Z. noltii* and dark material/shadow with 28% of *Z. noltii* pixels were incorrectly classed dark material/shadow within Transect A. All other benthic class combinations across all transect maps showed low misclassification cover ranging between 0% and 7.5%.

4 | DISCUSSION

4.1 | Habitat classification

This study aimed to evaluate a consumer-grade UAV multispectral camera for mapping a multispecies intertidal temperate seagrass environment. The objective was to discriminate between macroalgae and different *Zostera* spp., to capture accurate species-specific distribution patterns. This is essential for coastal managers to effectively address mitigating strategies for the prevention of seagrass species decline and the growth of detrimental macroalgae. Findings show that despite the complex environment and similar spectral

properties of *Zostera* spp. and green macroalgae, the five-band multispectral UAV camera and the MLC method can yield maps with overall accuracies (OA) ranging between 84% and 91%. When considering only the RGB bands, the OA was reduced by up to 28% across all transects. Likewise, PA and UA associated with vegetation classes declined substantially, highlighting the significant advantage that the red edge and near-infrared bands can provide to the effective mapping of an intertidal multispecies environment, increasing accuracy discriminating particularly between *Zostera* spp. and macroalgae. Although this provides the key to an operationally viable method for monitoring multispecies intertidal seagrass habitats, it is important to note that accuracies may decrease in subtidal areas or in areas where standing water is present due to absorption of light in the red edge and near-infrared wavelengths. However, the observed high OA here also aligns with prior studies that used 5–10 band multispectral UAVs to map intertidal seagrass-macroalgae environments. For example, in less complex intertidal seagrass-macroalgae environments, James et al. (2020) and Román et al. (2021) demonstrated an OA of 98.6% and 90.3%, respectively, using the MLC method. Holey et al. (2021) used a more sophisticated analysis, a deep learning method (Convolutional Neural Networks; FCNNs), in a similarly complex intertidal seagrass-macroalgae environment in LNNR and achieved an average accuracy of 88.4%, although without discriminating separate seagrass species. However, in comparison to the parametric method used in this study, recent studies have

demonstrated the efficacy of non-parametric classifiers, such as random forest (RF) and support vector machine (SVM), achieving notably higher accuracies (up to 98%) in similar seagrass environments (Chand & Bollard, 2022; Price et al., 2022), and as these approaches become more widely accessible in open source software, they have potential to provide improved operational mapping.

The three vegetation types, *Zostera* spp. and macroalgae were spectrally distinct across all investigated transects. This distinction may be attributed to their differences in leaf pigmentation enabling the discrimination between the different vegetation types (Davies et al., 2023; Fyfe, 2003). While *Z. noltii* and *Z. marina* have similar leaf pigmentation, opportunistic macroalgae (*Ulva intestinalis*), with its brighter pigmentation in green colour, indicated greater separability in comparison to that between *Z. noltii* and *Z. marina*. Notably, the peak reflectance of all vegetation types and a maximum separation in the spectral reflectance between *Zostera* spp. and macroalgae occurred in the green, red edge and near-infrared wavelength bands. These observations conform with generally observed spectral reflectance patterns in healthy plants that are known to absorb radiation in the blue and red wavelengths (around 450 and 670 nm, respectively) and reflect radiation in the green (around 530 nm), red edge and near-infrared wavelengths (around 730 and 840 nm, respectively) (Chand & Bollard, 2021; Davies et al., 2023; Schmidt & Skidmore, 2003). Although this study showed low spectral separability between *Z. noltii* and *Z. marina*, and higher misclassification between these two species, their separability could still be observed in the red edge and near-infrared bands. These results also align with Fyfe (2003) who showed that seagrass species could most easily be discriminated between 700 and 900 nm, and Davies et al. (2023), who demonstrated a steep reflectance signature from ~680 nm onwards for intertidal seagrass and algae. However, results contradict another study conducted by Román et al. (2021), who showed that the peak reflectance of *Z. noltii*, in an intertidal coastal area in Cadiz, Spain, was highest between 500 and 700 nm and declined from 700 nm. This difference may primarily stem from the absorption of near-infrared wavelengths by water in subtidal areas (Román et al., 2021; Tait et al., 2019), whereas for the intertidal environments in this study, the absence of a water column results in peak spectral reflectance in the near-infrared wavelengths. Other disparities between studies may be related to differences in spectral responses of seagrass due to, for example, the influence of epiphytes and epibionts (Fyfe, 2003; Hwang et al., 2019) or sediment background (Bargain et al., 2012).

A further advantage in creating accurate habitat maps from UAVs may be related to the ultra-high spatial resolution that the camera offers. The high resolution minimises mixed pixels (i.e., the representation of more than one class within a pixel). This may not only have aided in discriminating between the vegetation types (beyond the addition of red edge and near-infrared bands alone) but also reduced classification errors between vegetation types and non-vegetative classes. For example, when *Z. noltii* is found in sparse density, their thin leaves lie on the bare ground and could easily be misclassified with other benthic classes within the pixel when using a lower spatial resolution imagery, but this issue is avoidable if a pixel contains *Z. noltii* features entirely. Finally, high spatial resolution

imagery enables the identification of seagrass habitats to species level, which is critical to coastal managers for the monitoring of biodiversity and species distribution of seagrass.

4.2 | Limitations, challenges and recommendations

Although this study indicates high potential for using multispectral UAV imagery for mapping a complex multispecies intertidal seagrass environment, some limitations and challenges need to be considered from the planning stage and prior to flight missions of data collection, during field surveys and in the interpretation phases: (1) despite successful creation of multispecies seagrass habitat maps, results showed that some misclassification among vegetation is still likely and may impact the accuracy of species distribution maps, especially between the two *Zostera* spp. investigated in this study, and this may be of relevance for management applications when focusing on species-specific targeted protection or management; (2) the level of 'wetness' in the field site may vary according to tidal stage and weather conditions (e.g., sunny and cloudy), which may influence spectral signatures and make repeatability for comparisons challenging. To maximise comparable results, ideally similar tidal stages and weather conditions should be considered; (3) unfavourable environmental conditions can pose numerous challenges during field surveys and hamper logistics. In cases where the field site of interest cannot be surveyed outside the mudflat areas, such as in this study, similar to traditional field surveys, UAV surveys can remain challenging in terms of accessing areas with soft sediments on foot, with potential hazards of getting stuck in soft bottom areas; (4) protected site specific restrictions, for example, prohibition of surveys during the period of nesting and breeding birds, and foraging seasons, need to be considered to minimise impact on protected features, to avoid the potential collision of UAV with birds and disturbance to nesting birds; (5) given the restricted and limited periods of time during low tide available to conduct the surveys and that all the necessary conditions (e.g., wind speed and weather) to fly a UAV must be met within a particular time slot, a well-planned manageable operation is recommended for maximum efficiency and safety; (6) it is important to consider that large-scale mapping can be restricted due to short battery autonomy and Visual Line Of Sight (VLOS) restrictions, on flight altitude and distance (Nahirnick, Hunter, et al., 2019; Walker et al., 2023). In the UK, for example, the current flight limit is typically restricted to 120 m altitude and within VLOS, with further qualifications required when flying a UAV beyond these limits. To overcome this challenge, it is recommended to either have additional batteries on the field site or increase battery capacity by increasing flight altitude at the cost of lower spatial resolution; (7) other technological issues that may be encountered in the field can be related to GNSS accuracy. For example, GNSS signals can be blocked or weakened through cloud coverage and result in inaccurate positioning of ground-truth surveys and thus may impact the post-processing and map results and should be considered; (8) with improving technology and more cost-effective imaging tools developing, the methods and map accuracies in a spectrally complex intertidal environment could be enhanced by utilising UAV-based

hyperspectral sensors. For example, hyperspectral sensors mounted on a UAV can capture data across a wide range of wavelengths, enabling enhanced discrimination between spectrally similar vegetation classes and thus giving potential accuracy improvements (Banerjee et al., 2020; Rossiter et al., 2020). Incorporating additional data types, such as UAV laser scanning data, providing vegetation structure and topographic information, may also offer benefits for classification and for interpretation and modelling of vegetation distribution, and this remains little explored in this application area; (9) the utilisation of expensive software, including ArcGIS and ENVI, may limit accessibility for coastal managers due to budget constraints. To promote the reproducibility and cost-effectiveness of the production of habitat maps, open-source software such as QGIS and programming languages including R and Python may offer more affordable alternatives (Rocchini et al., 2017).

4.3 | Benefits for management

A major drawback of UAV-based habitat mapping for management and conservation applications lies in the relatively small areas UAVs are able to map, particularly in comparison to satellites. To derive maximum benefit from the utilisation of UAVs for effective seagrass mapping and monitoring, combining UAV strengths with the greater spatial coverage of satellite imagery may allow scalability in analysis and enable seagrass conservation efforts to be more effective across larger spatial scales and over time. For example, proposed methodologies could support effective management by overcoming expensive, time-consuming and exhaustive quadrat sampling in challenging mudflat environments by using UAV-derived classified transects as samples to assess the condition of seagrass habitats (Figure 5). UAV-derived maps can also be utilised as ground-truth for large-scale habitat mapping, using freely available satellite imagery to create broad-scale habitat maps for presence/absence and density maps (Carpenter et al., 2022; Lewis et al., 2023; Makri et al., 2018). Moreover, multispectral UAV-derived habitat maps could be developed as an integral part of multitemporal seagrass habitat monitoring, allowing for greater reproducibility and repeatability of habitat mapping (Prystay et al., 2023; Ventura et al., 2022). Finally, UAV-derived habitat maps may provide a foundation to develop effective communication tools used for decision and policy for seagrass habitat protection.

5 | CONCLUSIONS

This study demonstrates the viability of using an off-the-shelf multispectral UAV to accurately map a complex intertidal seagrass environment. While a traditional RGB UAV has been widely employed for seagrass habitat mapping, our findings show the advantages of a multispectral UAV for enhanced accuracy in mapping fine-scale, multispecies, seagrass-macroalgae habitats. The ultra-high image resolution and additional red edge and near-infrared bands enabled discrimination between vegetation classes at species level and,

ultimately, the creation of fine-scale habitat maps. Using a five-band camera and a user-friendly classifier, similar accuracy results can be achieved with a study that has, for example, applied more computationally intensive methods (e.g., Hobley et al., 2021). However, the additional number of spectral bands comes with some trade-offs, including increased data complexity associated with data processing, analysis, computational demands and required expertise in handling multispectral datasets. Moreover, the challenging environment of the mudflats requires careful fieldwork planning and consideration of optimal flight missions to ensure consistent environmental conditions during imagery acquisition for reliable and comparable results for an effective monitoring programme. Despite these challenges, we demonstrate the potential of a cost-effective approach in creating accurate multispecies intertidal seagrass habitat maps, which may be operationally more accessible to coastal managers. The study may provide a foundation for further investigation to aid coastal managers to develop effective monitoring programmes by integrating multispectral UAV-derived habitat maps in monitoring programmes. The methodology of this study can be utilised to implement targeted management practices to identify areas of concern and potential threats to effectively manage *Zostera* spp. decline and detrimental macroalgae growth.

AUTHOR CONTRIBUTIONS

Eylem Elma: Conceptualization; investigation; writing—original draft; methodology; visualization; writing—review and editing; formal analysis; data curation; funding acquisition. **Rachel Gaulton:** Writing—review and editing; supervision; validation. **Thomas R. Chudley:** Writing—review and editing; data curation. **Catherine L. Scott:** Funding acquisition; writing—review and editing; supervision; resources. **Holly K. East:** Writing—review and editing; supervision. **Hannah Westoby:** Writing—review and editing; supervision. **Clare Fitzsimmons:** Supervision; resources; project administration; software; validation; writing—review and editing; funding acquisition; conceptualization.

ACKNOWLEDGEMENTS

We thank Natural England and the management team of Lindisfarne National Nature Reserve (LNNR) for their invaluable local knowledge, shared experiences and logistical support during the surveys of this study. We would also like to thank all participants and volunteers who devoted their time to support in the field. We thank NERC Field Spectroscopy Facility (FSF) for funding and providing the spectral reflectance panel used in this study. This work was funded by the Natural Environment Research Council (NERC) via the ONE Planet DTP [NE/S007512/1] and Natural England, UK.

CONFLICT OF INTEREST STATEMENT

The authors declare no conflict of interest.

DATA AVAILABILITY STATEMENT

The data that support the findings of this study are available from the corresponding author upon reasonable request.

ETHICS STATEMENT

No ethical approval was required for this study. A permit to conduct field surveys in Lindisfarne National Nature Reserve (LNNR) was acquired from Natural England.

PERMISSION TO REPRODUCE MATERIAL FROM OTHER SOURCES

All material presented in this study is original. No permissions to reproduce material from other sources were required in this work.

ORCID

Eylem Elma  <https://orcid.org/0000-0001-8305-1169>

Thomas R. Chudley  <https://orcid.org/0000-0001-8547-1132>

REFERENCES

- Agisoft. (2021). Agisoft metashape user manual. In *Agisoft Metashape* (Issue September, p. 160). https://www.agisoft.com/pdf/metashape-pro_1_5_en.pdf
- Banerjee, B.P., Raval, S. & Cullen, P.J. (2020). UAV-hyperspectral imaging of spectrally complex environments. *International Journal of Remote Sensing*, 41(11), 4136–4159. <https://doi.org/10.1080/01431161.2020.1714771>
- Bargain, A., Robin, M., le Men, E., Huete, A. & Barillé, L. (2012). Spectral response of the seagrass *Zostera noltii* with different sediment backgrounds. *Aquatic Botany*, 98(1). <https://doi.org/10.1016/j.aquabot.2011.12.009>
- Bertelli, C.M. & Unsworth, R.K.F. (2014). Protecting the hand that feeds us: seagrass (*Zostera marina*) serves as commercial juvenile fish habitat. *Marine Pollution Bulletin*, 83(2). <https://doi.org/10.1016/j.marpolbul.2013.08.011>
- Bremner, J., Petus, C., Dolphin, T., Hawes, J., Beguet, B. & Devlin, M.J. (2023). A seagrass mapping toolbox for South Pacific environments. *Remote Sensing*, 15(3). <https://doi.org/10.3390/rs15030834>
- Burkholder, J.A.M., Tomasko, D.A. & Touchette, B.W. (2007). Seagrasses and eutrophication. *Journal of Experimental Marine Biology and Ecology*, 350(1–2). <https://doi.org/10.1016/j.jembe.2007.06.024>
- Cardoso, P.G., Pardal, M.A., Lillebø, A.I., Ferreira, S.M., Raffaelli, D. & Marques, J.C. (2004). Dynamic changes in seagrass assemblages under eutrophication and implications for recovery. *Journal of Experimental Marine Biology and Ecology*, 302(2). <https://doi.org/10.1016/j.jembe.2003.10.014>
- Carpenter, S., Byfield, V., Felgate, S.L., Price, D.M., Andrade, V., Cobb, E. et al. (2022). Using unoccupied aerial vehicles (UAVs) to map seagrass cover from Sentinel-2 imagery. *Remote Sensing*, 14(3). <https://doi.org/10.3390/rs14030477>
- Chand, S. & Bollard, B. (2021). Low altitude spatial assessment and monitoring of intertidal seagrass meadows beyond the visible spectrum using a remotely piloted aircraft system. *Estuarine, Coastal and Shelf Science*, 255. <https://doi.org/10.1016/j.ecss.2021.107299>
- Chand, S. & Bollard, B. (2022). Detecting the spatial variability of seagrass meadows and their consequences on associated macrofauna benthic activity using novel drone technology. *Remote Sensing*, 14(1). <https://doi.org/10.3390/rs14010160>
- Clausen, K.K., Clausen, P., Fællid, C.C. & Mouritsen, K.N. (2012). Energetic consequences of a major change in habitat use: endangered brent geese *branta bernicla hrota* losing their main food resource. *Ibis*, 154. <https://doi.org/10.1111/j.1474-919X.2012.01265.x>
- Congalton, R.G. & Green, K. (2008). *Assessing the accuracy of remotely sensed data: principles and practices*. 2nd edition, Boca Raton: Lewis Publishers.
- Davies, B.F.R., Gernez, P., Oiry, S., Rosa, P., Zoffoli, M.L. & Barill, L. (2023). Multi- and hyperspectral classification of soft-bottom intertidal vegetation using a spectral library for coastal biodiversity remote sensing. *Remote Sensing of Environment*, 290, 113554. <https://doi.org/10.1016/j.rse.2023.113554>
- Doukari, M. & Topouzelis, K. (2022). Overcoming the UAS limitations in the coastal environment for accurate habitat mapping. *Remote Sensing Applications: Society and Environment*, 26, 100726. <https://doi.org/10.1016/j.rsase.2022.100726>
- Duffy, J.P., Pratt, L., Anderson, K., Land, P.E. & Shutler, J.D. (2018). Spatial assessment of intertidal seagrass meadows using optical imaging systems and a lightweight drone. *Estuarine, Coastal and Shelf Science*, 200. <https://doi.org/10.1016/j.ecss.2017.11.001>
- Duníc, J.C., Brown, C.J., Connolly, R.M., Turschwell, M.P. & Côté, I.M. (2021). Long-term declines and recovery of meadow area across the world's seagrass bioregions. *Global Change Biology*, 27. <https://doi.org/10.1111/gcb.15684>
- Fyfe, S.K. (2003). Spatial and temporal variation in spectral reflectance: are seagrass species spectrally distinct? *Limnology and Oceanography*, 48. https://doi.org/10.4319/lo.2003.48.1_part_2.0464
- Ganter, B. (2000). Seagrass (*Zostera* spp.) as food for brent geese (*Branta bernicla*): an overview. *Helgoland Marine Research*, 54. <https://doi.org/10.1007/s101520050003>
- Gao, G., Beardall, J., Jin, P., Gao, L., Xie, S. & Gao, K. (2022). A review of existing and potential blue carbon contributions to climate change mitigation in the Anthropocene. *Journal of Applied Ecology*, 59. <https://doi.org/10.1111/1365-2664.14173>
- Grech, A., Chartrand-Miller, K., Erftemeijer, P., Fonseca, M., McKenzie, L., Rasheed, M. et al. (2012). A comparison of threats, vulnerabilities and management approaches in global seagrass bioregions. *Environmental Research Letters*, 7, 024006. <https://doi.org/10.1088/1748-9326/7/2/024006>
- Green, A.E., Unsworth, R.K.F., Chadwick, M.A. & Jones, P.J.S. (2021). Historical analysis exposes catastrophic seagrass loss for the United Kingdom. *Frontiers in Plant Science*, 12. <https://doi.org/10.3389/fpls.2021.629962>
- Hauxwell, J., Cebrián, J., Furlong, C. & Valiela, I. (2001). Macroalgal canopies contribute to eelgrass (*Zostera marina*) decline in temperate estuarine ecosystems. *Ecology*, 82(4). <https://doi.org/10.2307/2679899>
- Hobley, B., Arosio, R., French, G., Bremner, J., Dolphin, T. & Mackiewicz, M. (2021). Semi-supervised segmentation for coastal monitoring seagrass using RPA imagery. *Remote Sensing*, 13(9). <https://doi.org/10.3390/rs13091741>
- Hossain, M.S., Bujang, J.S., Zakaria, M.H. & Hashim, M. (2015). The application of remote sensing to seagrass ecosystems: an overview and future research prospects. *International Journal of Remote Sensing*, 36(1). <https://doi.org/10.1080/01431161.2014.990649>
- Hughes, A.R., Williams, S.L., Duarte, C.M., Heck, K.L. & Waycott, M. (2009). Associations of concern: declining seagrasses and threatened dependent species. *Frontiers in Ecology and the Environment*, 7(5). <https://doi.org/10.1890/080041>
- Hwang, C., Chang, C.H., Kildea, T., Burch, M. & Fernandes, M. (2019). Effects of epiphytes and depth on seagrass spectral profiles: case study of gulf St. Vincent, South Australia. *International Journal of Environmental Research and Public Health*, 16(15). <https://doi.org/10.3390/ijerph16152701>
- James, D., Collin, A., Houet, T., Mury, A., Gloria, H. & le Poulain, N. (2020). Towards better mapping of seagrass meadows using UAV multispectral and topographic data. *Journal of Coastal Research*, 95(sp1). <https://doi.org/10.2112/SI95-217.1>
- Jones, B.L., Cullen-Unsworth, L.C. & Unsworth, R.K.F. (2018). Tracking nitrogen source using $\delta^{15}N$ reveals human and agricultural drivers of seagrass degradation across the British Isles. *Frontiers in Plant Science*, 9, 133. <https://doi.org/10.3389/fpls.2018.00133>

- Jones, B.L. & Unsworth, R.K.F. (2016). The perilous state of seagrass in the British Isles. *Royal Society Open Science*, 3, 150596. <https://doi.org/10.1098/rsos.150596>
- Kaldy, J.E. (2014). Effect of temperature and nutrient manipulations on eelgrass *Zostera marina* L. from the Pacific Northwest, USA. *Journal of Experimental Marine Biology and Ecology*, 453. <https://doi.org/10.1016/j.jembe.2013.12.020>
- la Nafie, Y.A., de los Santos, C.B., Brun, F.G., van Katwijk, M.M. & Bouma, T.J. (2012). Waves and high nutrient loads jointly decrease survival and separately affect morphological and biomechanical properties in the seagrass *Zostera noltii*. *Limnology and Oceanography*, 57(6). <https://doi.org/10.4319/lo.2012.57.6.1664>
- Lewis, P.H., Roberts, B.P., Moore, P.J., Pike, S., Scarth, A., Medcalf, K. et al. (2023). Combining unmanned aerial vehicles and satellite imagery to quantify areal extent of intertidal brown canopy-forming macroalgae. *Remote Sensing in Ecology and Conservation*, 9(4), 540–552. <https://doi.org/10.1002/rse2.32>
- Maier, G., Nimmo-Smith, R.J., Glegg, G.A., Tappin, A.D. & Worsfold, P.J. (2009). Estuarine eutrophication in the UK: current incidence and future trends. *Aquatic Conservation: Marine and Freshwater Ecosystems*, 19, 43–56. <https://doi.org/10.1002/aqc>
- Makri, D., Stamatis, P., Doukari, M., Papakonstantinou, A., Vasilakos, C. & Topouzelis K. (2018). Multi-scale seagrass mapping in satellite data and the use of UAS in accuracy assessment, Proc. SPIE 10773, Sixth International Conference on Remote Sensing and Geoinformation of the Environment (RSCy2018), 107731T. <https://doi.org/10.1117/12.23260012>
- Martin, R., Ellis, J., Brabyn, L. & Campbell, M. (2020). Change-mapping of estuarine intertidal seagrass (*Zostera muelleri*) using multispectral imagery flown by remotely piloted aircraft (RPA) at Wharekawa Harbour, New Zealand. *Estuarine, Coastal and Shelf Science*, 246, 107046. <https://doi.org/10.1016/j.ecss.2020.107046>
- Massa, S.I., Arnaud-Haond, S., Pearson, G.A. & Serrão, E.A. (2009). Temperature tolerance and survival of intertidal populations of the seagrass *Zostera noltii* (Hornemann) in Southern Europe (Ria Formosa, Portugal). *Hydrobiologia*, 619. <https://doi.org/10.1007/s10750-008-9609-4>
- Nahirnack, N.K., Hunter, P., Costa, M., Schroeder, S. & Sharma, T. (2019). Benefits and challenges of UAS imagery for eelgrass (*Zostera marina*) mapping in small estuaries of the Canadian West Coast. *Journal of Coastal Research*, 35(3), 673. <https://doi.org/10.2112/jcoastres-d-18-00079.1>
- Nahirnack, N.K., Reshitnyk, L., Campbell, M., Hessing-Lewis, M., Costa, M., Yakimishyn, J. et al. (2019). Mapping with confidence; delineating seagrass habitats using Unoccupied Aerial Systems (UAS). *Remote Sensing in Ecology and Conservation*, 5(2). <https://doi.org/10.1002/rse2.98>
- Orth, R.J., Carruthers, T.J.B., Dennison, W.C., Duarte, C.M., Fourqurean, J.W., Heck, J.R. et al. (2006). A global crisis for seagrass ecosystems. *Bioscience*, 56(12). [https://doi.org/10.1641/0006-3568\(2006\)56\[987:agcfse\]2.0.co;2](https://doi.org/10.1641/0006-3568(2006)56[987:agcfse]2.0.co;2)
- Over, J.-S.R., Ritchie, A.C., Kranenburg, C.J., Jenna A.B, Buscombe, D., Noble, T., Sherwood, C.R., Warrick, J.A. & Wernette, P.A. (2021). Processing Coastal Imagery With Agisoft Metashape Professional Edition, Version 1. 6 – Structure From Motion Workflow Documentation. <https://pubs.usgs.gov/of/2021/1039/ofr20211039.pdf>
- Polte, P. & Asmus, H. (2006). Intertidal seagrass beds (*Zostera noltii*) as spawning grounds for transient fishes in the Wadden Sea. *Marine Ecology Progress Series*, 312. <https://doi.org/10.3354/meps312235>
- Postlethwaite, V.R., McGowan, A.E., Kohfeld, K.E., Robinson, C.L.K. & Pellatt, M.G. (2018). Low blue carbon storage in eelgrass (*Zostera marina*) meadows on the Pacific coast of Canada. *PLoS ONE*, 13(6). <https://doi.org/10.1371/journal.pone.0198348>
- Price, D.M., Felgate, S.L., Huvenne, V.A.I., Strong, J., Carpenter, S., Barry, C. et al. (2022). Quantifying the intra-habitat variation of seagrass beds with Unoccupied Aerial Vehicles (UAVs). *Remote Sensing*, 14(3). <https://doi.org/10.3390/rs14030480>
- Prystay, T.S., Adams, G., Favaro, B., Gregory, R.S. & le Bris, A. (2023). The reproducibility of remotely piloted aircraft systems to monitor seasonal variation in submerged seagrass and estuarine habitats. *Facets*, 8(1). <https://doi.org/10.1139/facets-2022-0149>
- Richards, J.A. (2013). Remote sensing digital image analysis. In: *Remote sensing digital image analysis*, 5th edition, Berlin Heidelberg: Springer. <https://doi.org/10.1007/978-3-662-03978-6>
- Rocchini, D., Petras, V., Petrasova, A., Horning, N., Furtkevicova, L., Neteler, M. et al. (2017). Open data and open source for remote sensing training in ecology. *Ecological Informatics*, 40, 57–61. <https://doi.org/10.1016/j.ecoinf.2017.05.004>
- Röhr, M.E., Holmer, M., Baum, J.K., Björk, M., Chin, D., Chalifour, L. et al. (2018). Blue carbon storage capacity of temperate eelgrass (*Zostera marina*) meadows. *Global Biogeochemical Cycles*, 32. <https://doi.org/10.1029/2018GB005941>
- Román, A., Tovar-Sánchez, A., Olivé, I. & Navarro, G. (2021). Using a UAV-mounted multispectral camera for the monitoring of marine macrophytes. *Frontiers in Marine Science*, 8. <https://doi.org/10.3389/fmars.2021.722698>
- Rossiter, T., Furey, T., McCarthy, T. & Stengel, D.B. (2020). UAV-mounted hyperspectral mapping of intertidal macroalgae. *Estuarine, Coastal and Shelf Science*, 242, 106789. <https://doi.org/10.1016/j.ecss.2020.106789>
- Schmidt, K.S. & Skidmore, A.K. (2003). Spectral discrimination of vegetation types in a coastal wetland. *Remote Sensing of Environment*, 85. [https://doi.org/10.1016/S0034-4257\(02\)00196-7](https://doi.org/10.1016/S0034-4257(02)00196-7)
- Sousa, A.I., da Silva, J.F., Azevedo, A. & Lillebø, A.I. (2019). Blue carbon stock in *Zostera noltei* meadows at Ria de Aveiro coastal lagoon (Portugal) over a decade. *Scientific Reports*, 9, 14387. <https://doi.org/10.1038/s41598-019-50425-4>
- Strachan, L.L., Lilley, R.J. & Hennige, S.J. (2022). A regional and international framework for evaluating seagrass management and conservation. *Marine Policy*, 146, 105306. <https://doi.org/10.1016/j.marpol.2022.105306>
- Svane, N., Lange, T., Egemose, S., Dalby, O., Thomasberger, A. & Flindt, M.R. (2022). Unoccupied aerial vehicle-assisted monitoring of benthic vegetation in the coastal zone enhances the quality of ecological data. *Progress in Physical Geography*, 46(2). <https://doi.org/10.1177/0309133211052005>
- Tahara, S., Sudo, K., Yamakita, T. & Nakaoka, M. (2022). Species level mapping of a seagrass bed using an unmanned aerial vehicle and deep learning technique. *PeerJ*, 10, e14017. <https://doi.org/10.7717/peerj.14017>
- Tait, L., Bind, J., Charan-Dixon, H., Hawes, I., Pirker, J. & Schiel, D. (2019). Unmanned aerial vehicles (UAVs) for monitoring macroalgal biodiversity: comparison of RGB and multispectral imaging sensors for biodiversity assessments. *Remote Sensing*, 11(19). <https://doi.org/10.3390/rs11192332>
- Turschwell, M.P., Connolly, R.M., Dunic, J.C., Sievers, M., Buelow, C.A., Pearson, R.M. et al. (2021). Anthropogenic pressures and life history predict trajectories of seagrass meadow extent at a global scale. *Proceedings of the National Academy of Sciences of the United States of America*, 118(45). <https://doi.org/10.1073/pnas.2110802118>
- United Nations Environment Programme (UNEP). (2020). Out of blue: the value of seagrasses to the environment and to people.
- Unsworth, R.K.F., Cullen-Unsworth, L.C., Jones, B.L.H. & Lilley, R.J. (2022). The planetary role of seagrass conservation. *Science*, 377, 6606. <https://doi.org/10.1126/science.abq6923>
- Unsworth, R.K.F., McKenzie, L.J., Collier, C.J., Cullen-Unsworth, L.C., Duarte, C.M., Eklöf, J.S. et al. (2019). Global challenges for seagrass conservation. *Ambio*, 48. <https://doi.org/10.1007/s13280-018-1115-y>

- Veettil, B.K., Ward, R.D., Lima, M.D.A.C., Stankovic, M., Hoai, P.N. & Quang, N.X. (2020). Opportunities for seagrass research derived from remote sensing: a review of current methods. *Ecological Indicators*, 117, 106560. <https://doi.org/10.1016/j.ecolind.2020.106560>
- Ventura, D., Bonifazi, A., Gravina, M.F., Belluscio, A. & Ardizzone, G. (2018). Mapping and classification of ecologically sensitive marine habitats using unmanned aerial vehicle (UAV) imagery and Object-Based Image Analysis (OBIA). *Remote Sensing*, 10(9). <https://doi.org/10.3390/rs10091331>
- Ventura, D., Mancini, G., Casoli, E., Pace, D.S., Lasinio, G.J., Belluscio, A. et al. (2022). Seagrass restoration monitoring and shallow-water benthic habitat mapping through a photogrammetry-based protocol. *Journal of Environmental Management*, 304, 114262. <https://doi.org/10.1016/j.jenvman.2021.114262>
- Walker, S.E., Sheaves, M. & Waltham, N.J. (2023). Barriers to using UAVs in conservation and environmental management: a systematic review. *Environmental Management*, 71. <https://doi.org/10.1007/s00267-022-01768-8>
- Waycott, M., Duarte, C.M., Carruthers, T.J.B., Orth, R.J., Dennison, W.C., Olyarnik, S. et al. (2009). Accelerating loss of seagrasses across the globe threatens coastal ecosystems. *Proceedings of the National Academy of Sciences of the United States of America*, 106(30). <https://doi.org/10.1073/pnas.0905620106>
- Wilson, K., Pressey, R.L., Newton, A., Burgman, M., Possingham, H. & Weston, C. (2005). Measuring and incorporating vulnerability into conservation planning. *Environmental Management*, 35. <https://doi.org/10.1007/s00267-004-0095-9>
- Yang, B., Hawthorne, T.L., Aoki, L., Beatty, D.S., Copeland, T., Domke, L.K. et al. (2023). Low-altitude UAV imaging accurately quantifies eelgrass wasting disease from Alaska to California. *Geophysical Research Letters*, 50, e2022GL101985. <https://doi.org/10.1029/2022GL101985>
- Yang, B., Hawthorne, T.L., Hessing-Lewis, M., Duffy, E.J., Reshitnyk, L.Y., Feinman, M. et al. (2020). Developing an introductory UAV/drone mapping training program for seagrass monitoring and research. *Drones*, 4(4). <https://doi.org/10.3390/drones4040070>
- Zou, Y.F., Chen, K.Y. & Lin, H.J. (2021). Significance of belowground production to the long-term carbon sequestration of intertidal seagrass beds. *Science of the Total Environment*, 800, 149579. <https://doi.org/10.1016/j.scitotenv.2021.149579>

How to cite this article: Elma, E., Gaulton, R., Chudley, T.R., Scott, C.L., East, H.K., Westoby, H. et al. (2024). Evaluating UAV-based multispectral imagery for mapping an intertidal seagrass environment. *Aquatic Conservation: Marine and Freshwater Ecosystems*, 34(8), e4230. <https://doi.org/10.1002/aqc.4230>